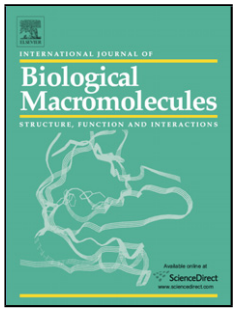

Title: Evaluation of DNA/Protein interactions and cytotoxic studies of copper(II) complexes incorporated with N, N donor ligands and terpyridine ligand

Author: Tummalapalli Kiran C.S. Vasavi Punnagai Munusami Madhvesh Pathak M.M. Balamurali

PII: S0141-8130(16)30969-2
DOI: http://dx.doi.org/doi:10.1016/j.ijbiomac.2016.11.022
Reference: BIOMAC 6709

To appear in: *International Journal of Biological Macromolecules*

Received date: 23-7-2016
Revised date: 2-11-2016
Accepted date: 3-11-2016

Please cite this article as: Tummalapalli Kiran, C.S.Vasavi, Punnagai Munusami, Madhvesh Pathak, M.M.Balamurali, Evaluation of DNA/Protein interactions and cytotoxic studies of copper(II) complexes incorporated with N, N donor ligands and terpyridine ligand, International Journal of Biological Macromolecules http://dx.doi.org/10.1016/j.ijbiomac.2016.11.022

Evaluation of DNA/Protein interactions and cytotoxic studies of copper(II) complexes incorporated with N, N donor ligands and terpyridine ligand

Tummalapalli Kiran[a], C. S Vasavi[b], Punnagai Munusami[c], Madhvesh Pathak*[a], Balamurali M M †[a]

[a] *Department of Chemistry, School of Advanced Sciences, VIT University, Vellore, Tamilnadu 632014, India.*
[b] *Bioinformatics Division, School of Bio Sciences and Technology, VIT University, Vellore, Tamil Nadu 632 014, India.*
[c] *Center for Computational Natural Sciences and Bioinformatics, International Institute of Information Technology, Hyderabad 500 032, India.*

* Corresponding author. Tel.: +91-416-2202553; E-mail: madhveshpathak@vit.ac.in (M. Pathak) †
Co-corresponding author. Tel.: +91-416-2202321. E-mail: balamurali.mm@vit.ac.in (Balamurali M M)

Graphical abstract

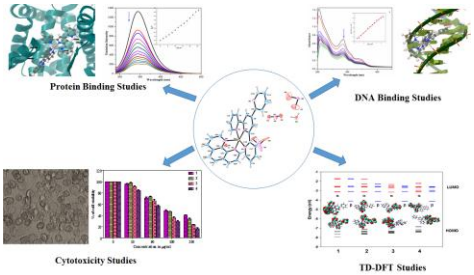

A series of four new heteroleptic derivatives of copper(II) synthesized and structurally characterized as a distorted square-pyramidal geometry around central metal. Significant biological applications e.g. DNA interactions, protein binding, molecular docking, Density Functional Theory (DFT) calculations and cytotoxicity of these complexes exhibited their noted worth.

Highlights

- A series of four metallo-organic complexes of copper(II) have been synthesized.
- Physico-chemical characterization techniques established very well and penta coordinated, distorted square-pyramidal geometry with triclinic system was confirmed by single crystal X-ray diffraction technique.
- DNA and protein binding studies displayed the mode of binding in an elaborative fashion.
- Molecular docking and Density Functional Theory (DFT) calculations are providing additional essential features of these new derivatives
- All the complexes have been carried out for cytotoxic studies with fruitful results

Abstract

A series of four new copper(II) heteroleptic complexes, [Cu(2‴-pytpy) (L)] $(NO_3)_2.2H_2O$ (**1-4**), where 2‴-pytpy= 4′-(2‴-Pyridyl)-2, 2′:6′, 2″-terpyridine, L=bipyridyl (bpy), 1, 10 phenanthroline(phen), dipyridoquinoxaline(dpq) and dipyridophenazine (dppz) were synthesized and characterized by spectroscopic techniques. Further, the molecular structure of the complex (2) was confirmed by single crystal X-ray diffraction technique and the data revealed a penta coordinated, distorted square-pyramidal geometry with triclinic system. The interactions of four complexes with calf thymus DNA and bovine serum albumin (BSA) were investigated by electronic absorption, fluorescence and circular dichroism spectroscopy techniques. Spectral studies substantiated an intercalative binding mode of metal complexes with ct-DNA. Significant binding interactions of the complexes with protein have been further revealed from fluorescence studies. Furthermore, all the four complexes show potential cytotoxicity towards the human liver carcinoma cell line (HepG-2).

Keywords: Copper(II) complexes, DNA and protein binding studies, Molecular docking, Density Functional Theory (DFT) calculations and Cytotoxicity studies.

1. Introduction

Along the path towards innovative progress for the treatment of cancer, the metal-based organic compounds are being intensively explored for the past several decades. Though cis-platin is popularly known as an anti-cancer drug since 1978 [1-3], the antitumor activity of second generation platinum complexes have been identified and thoroughly studied for their structure activity relationships while designing drug molecules [4, 5]. An in-depth investigation on the structure and activity of new organic probes have gained their significance despite the fact that DNA and proteins are the preliminary targets for anticancer drugs. The molecule which acts as target selective agent for DNA/protein mainly depends on the structure of the ligand, nature of functional groups and metal centers thereby mimicking the biological enzymes or endonucleases [6]. Recent days metal complex based anticancer agents, with potential in vitro toxicity have gained immense importance [7, 8]. As it is proven that platinum-based drugs show cellular resistance and undesirable side effects [9-11], much efforts are made to develop non-platinum based anticancer agents with bio-essential metal ions such as zinc(II), copper(II) and iron(III) were found to be successful [12-15]. These new metal complexes are known to have strong influence on the structural and conformational changes of DNA and protein inside the cell.

Copper is the third most abundant transition metal present in the cellular body after iron and zinc [16-18]. Enzymes like dismutase (containing copper) have their key roles in maintaining cellular metabolic wastes [19, 20]. Recently, derivatives of above-said metals incorporated with terpyridine were reported as potent chemotherapeutic drugs [21, 22]. Fine tuning and selectivity of the drug molecule depends on substitutions of the ligand that coordinates with the metal center. Moreover, it is quite obvious that the nature of the ligand plays an important role in the binding of metal complexes to the bio molecules.

Metal complexes having extended planarity tend to bind with DNA intercalatively [23]. However, metal complexes with ligands lacking planar structure are also reported to bind with DNA through non-intercalative mode [24]. The central metal ion is also expected to play a role in determining the efficacy of the metal complexes e. g. a redox active metal ion such as Cu(II) may promote transformation of a biomolecule through an oxidative pathway [25]. On account of these descriptions and expandable potentials, copper based complexes have been investigated in the present work and the new observations make additional contributions to the field concerned. In

this work an attempts have been made to understand the effect of metal ions with heteroleptic ligands like terpyridine and phenanthroline with extended planarity. The DNA binding ability and the cytotoxicity of these complexes have also been investigated.

2. Experimental

2.1. Materials

Deoxyribonucleic acid sodium salt from calf thymus, 2-acetyl pyridine, 2-pyridine-carboxaldehyde, bipyridyl and 1, 10 phenanthroline monohydrate were obtained from Sigma Aldrich. All the solvents and copper(II) nitrate trihydrate were procured commercially (SDFCL) and used without further purification. All the buffer solutions were prepared by using Millipore Water and pH was maintained in the range of 7.2-7.4. The ancillary ligands dipyrido [3, 2-*d*: 2′, 3′-*f*]-quinoxaline (dpq), and dipyrido [3, 2-*a*: 2′, 3′-*c*] phenazine (dppz) were prepared as reported elsewhere [26].

2.2. Instrumentation

The ^{1}H and ^{13}C magnetic resonance spectral data were recorded on a Bruker Avance III-400 MHz spectrometer, using $CDCl_3$ as solvent and Trimethylsilane (TMS) as an internal standard. UV-Vis absorption spectra were obtained using Jasco v-670 UV-VIS-NIR spectrophotometer. FT-IR spectra of ligands and new complexes were recorded as KBr pellets on a Shimadzu IR affinity-1 spectrophotometer in the range of 4000-400 cm^{-1}. The elemental analysis (C, H, N, O) of metal complexes were performed on Elementar Vario EL III analyzer. The molecular weight of ligand and complexes were ensured from Agilent Technologies 6310 Ion Trap LC/MS with 1200 Series. Fluorescence emission spectra were obtained from Hitachi F-7000FL spectrometer. Circular dichroism studies for ct-DNA and protein (BSA) with metal complexes were measured on a circular dichroism spectropolarimeter JASCO-J717 under nitrogen flush and 1 cm Quartz cell at 0.4 nm intervals in the wavelength range of 200-300 nm.

2.3. Preparation of 4′-(2‴-Pyridyl)-2, 2′:6′, 2″-terpyridine ligand

The ligand 4′-(2‴-pyridyl)-2, 2′:6′, 2″-terpyridine was prepared as reported in the literature [27]. 2-Acetyl pyridine (20.0 mmol, 2.24 ml) was added drop wise to an ethanolic solution of 2-pyridinecarboxaldehyde (10.0 mmol, 0.95 ml) containing potassium hydroxide (10.0 mmol, 0.77 g) and 30 % aqueous ammonia (80.0 mmol, 5 ml) under stirring conditions. The resultant dark brownish-yellow colored solution was stirred vigorously for 8h in ambient condition to get precipitated. The precipitate was collected, filtered and washed several times with distilled water followed by cold ethanol. An off white solid obtained was dried under vacuum and recrystallized using chloroform-methanol system.

Yield: 53% (1.62g, 6.4mmol) off white solid, m.p. 231-233 °C. IR (KBr cm^{-1}): 3053 w, 3010 w, 1581 s, 1546 m, 1467 m, 1390 m, 1259 w, 1070 w, 991 m, 777 s. UV–vis [(λ_{max} (nm), ε (L mol^{-1} cm^{-1})]: 206 (35,160), 242 (41,565), 280 (42,745), 316 (11,945). ^{1}H NMR ($CDCl_3$, 400MHz): δ (ppm): 7.36-7.33 (m, 3H, CH_{Ar}), 7.89-7.81(m, 3H, CH_{Ar}), 8.08-8.06 (d, J= 8Hz, 1H, CH_{Ar}), 8.67-8.65 (d, J=8Hz, 2H, CH_{Ar}), 8.75-8.73 (m, 2H, CH_{Ar}), 8.81-8.79 (m, 1H, CH_{Ar}), 9.10 (s, 2H, CH_{Ar}). ^{13}C NMR ($CDCl_3$, 100MHz): δ (ppm): 118.63, 121.28, 121.32, 123.72, 123.83, 136.83, 136.87, 148.64, 149.20, 150.04, 155.11, 156.21, 156. 25. ESI-MS: found: 311.4 (M+1), calcd: 310.12.

*2.4. Synthesis of [Cu(2‴-pytpy) (B)] $(NO_3)_2.2H_2O$ (B = bpy, **1**; phen, **2**; dpq, **3**; dppz, **4**)*

All the complexes were prepared by stirring a methanolic solution of $Cu(NO_3)_2.3H_2O$ (1.0 mmol, 241mg) with *2‴*-pytpy (1.0 mmol, 310mg) at room temperature for 30 min. Subsequently, methanolic solution of ancillary ligand B (1.0 mmol of bpy (156mg)/ phen (180mg)/ dpq (232mg)/ dppz (282mg)) was added drop wise into the former solution of copper salt and continued stirring for 3h. The obtained reaction mixture was filtered and kept aside for slow evaporation. Later solid products (accordingly) were isolated as blue (**1**, **2** and **3**), green (**4**) and were washed with diethyl ether followed by drying under vacuum. The crystallization of complex **2** for X-ray diffraction was processed in acetonitrile.

*[Cu(2‴-pytpy) (bpy)] $(NO_3)_2.2H_2O$ (**1**)*. Yield: 82%. Light blue crystalline solid. M.p.:217-219 °C Anal. Calc. for $C_{30}H_{26}CuN_8O_8$: C, 52.91; H, 3.80; N, 16.24; O, 18.55. Found: C, 52.84; H, 3.97; N, 16.37; O, 18.14. UV-Vis (methanol): λmax, nm (ε, $dm^3mol^{-1}cm^{-1}$) 220

(135150), 288 (34695), 334 (9240), 348 (8484). FT-IR (KBr phase, ν cm^{-1}): 3387 br, 3057 w, 1616 m, 1560 m, 1498 m, 1473 m, 1384 vs, 1274 w, 1022 w, 898 w, 839 w, 785 s, 729 w, 657 w, 493 w, 416 w (br, broad; vs, very strong; s, strong; m, medium; w, weak). LC-MS: found: 531(M+2), calcd: 529.12.

[Cu(2‴-pytpy) (phen)] $(NO_3)_2.2H_2O$ ***(2)***. Yield: 78%. Blue crystalline solid. M.p.:221-223 °C Anal. Calc. for $C_{32}H_{26}CuN_8O_8$: C, 53.82; H, 3.67; N, 15.69; O, 17.92. Found: C, 53.73; H, 3.61; N, 16.07; O, 17.86. UV-Vis (methanol): λmax, nm (ε, $dm^3mol^{-1}cm^{-1}$) 222 (141850), 266 (44900), 288 (38000), 344 (11465), 348 (9910). FT-IR (KBr phase, ν cm^{-1}): 3371 br, 3059 w, 1616 m, 1516 m, 1475 m, 1384 vs, 1244 w, 1018 m, 893 w, 848 m, 783 s, 725 s, 655 w, 497 w. LC-MS: found:554 (M+1), calcd: 553.12.

[Cu(2‴-pytpy) (dpq)] $(NO_3)_2.2H_2O$ ***(3)***. Yield: 82%. Dark blue crystalline solid. M.p.:266-268 °C Anal. Calc. for $C_{34}H_{26}CuN_{10}O_8$: C, 53.30; H, 3.42; N, 18.28; O, 16.71. Found: C, 53.27; H, 3.49; N, 18.36; O, 16.67. UV-Vis (methanol): λmax, nm (ε, $dm^3mol^{-1}cm^{-1}$) 222 (144230), 252 (49600), 288 (46390), 334 (15860), 348 (12745). FT-IR (KBr phase, ν cm^{-1}): 3327 br, 3057 w, 1614 m, 1554 w, 1471 m, 1384 vs, 1244 w, 1159 w, 1083 w, 1018 w, 898 w, 827 w, 783 s, 727 w, 655 m, 497 w, 437 w. LC-MS: found:606 (M+1), calcd: 605.13.

[Cu(2‴-pytpy) (dppz)] $(NO_3)_2.2H_2O$ ***(4)***. Yield: 82%. Green crystalline solid. M.p.: 273-275 °C Anal. Calc. for $C_{38}H_{28}CuN_{10}O_8$: C, 55.92; H, 3.46; N, 17.16; O, 15.68. Found: C, 55.84; H, 3.51; N, 17.23; O, 15.71. UV-Vis (methanol): λmax, nm (ε, $dm^3mol^{-1}cm^{-1}$) 226 (140350), 288 (27920), 334 (9320), 348 (8825). FT-IR (KBr phase, ν cm^{-1}): 3439 br, 3062 w, 1604 m, 1560 m, 1473 m, 1384 vs, 1251 w, 1157 m, 785 s, 725 m, 655 m, 617 w, 497 w, 418 w. LC-MS: found:657 (M+2), calcd: 655.14.

2.5 Single crystal X-ray crystallographic data collection and refinement of the structure

All the complexes were subjected for crystallization by slow evaporation technique. The single crystal X-ray diffraction analysis of complex **2** was performed on Bruker X8 Kappa APEXII diffractometer using graphite filter monochromatic MoKα radiation (λ=0.71073 A°) at 23°C with crystal dimension of 0.250×0.200×0.100 mm^3. The complex structure (**2**) was resolved by using SHELX-97 program [28] and all non-hydrogen atoms were solved with anisotropic thermal parameters by full matrix least squares refinement on F2 using

SHELX-97 software. The structure was partially solved by using direct method and converged to reliable structure using full matrix least square method. The final reliability index is 0.055. The hydrogen atoms were added geometrically and refined (using riding model) with fixed isotropic thermal parameters. The copper(II) complexes crystallize in triclinic with Centro-symmetric space group (P1).

2.6 Theoretical calculations

Gaussian 09 program [29] was used for the Density Functional Theory (DFT) calculations for all the copper complexes **1-4**. The complexes were fully optimized in the electronic ground state (S_0) using the three-parameter hybrid functional B3LYP. The standard basis sets LANL2DZ were used for Cu, 6-31+G** for N and 6-31G* for C and H. The optimized geometries of copper complexes **1-4** were verified for the absence of negative frequencies by performing frequency calculations. Table 1 summarizes the optimized molecular structure parameters in the ground state (S_0) for the complex **1-4**. In order to obtain the estimates of the vertical electron excitation energies, time-dependent density functional theory (TD-DFT; includes electron correlation) was performed on the calculated S_0 geometries using same B3LYP method and basis set [30, 31]. The solvent (methanol) effect was simulated using the polarizable continuum model with the integral equation formalism (IEF-PCM). Natural bond orbital (NBO) calculations were carried out with the NBO code included in GAUSSIAN-09. All the excitation energies, oscillator strength and the corresponding HOMO and LUMO contributions from all the electronic transitions are given in Table S3†.

2.7 DNA binding studies

In order to determine the binding interactions of newly synthesized metal complexes with ct-DNA, absorption spectral titration was carried out in 5 mM tris-HCl buffer (pH-7.2). The protein free form of ct-DNA was confirmed by the ratio of UV absorbance at 260 and 280 nm (A_{260}/A_{280}) of ca. 1.8 [32]. The concentration of ct-DNA per nucleotide was determined by its molar absorption coefficient (6600 m^{-1}) at 260 nm [33]. Stock solutions of metal complexes were prepared in DMF and further dilutions were made in 5 mM Tris-HCl buffer. The binding experiments were carried out with fixed concentration of the complex

(20 μM) and increasing concentrations of ct-DNA (0–26 μM) in both reference and sample solutions to nullify the absorbance peak of ct-DNA.

The competitive binding of metal complexes with ethidium bromide bound ct-DNA is explored by fluorescence spectroscopic technique. Solutions of EtBr and ct-DNA each at 5 μM concentration were prepared in 5 mM Tris-HCl buffer (pH-7.2), incubated for 1 hour at room temperature before being used for fluorescence experiments. The ethidium bromide bound ct-DNA was used as the reference solution. 515 nm and 597 nm were used as excitation and emission wavelengths, respectively. The reference solution (EtBr-DNA) is titrated against different concentrations of metal complexes (0–20 μM).

The stock solution of BSA (10 μM) was prepared in 50 mM phosphate buffer (pH-7.2) and stored at 4 °C until used. The binding mechanism of newly synthesized metal complexes with BSA (10 μM) were determined by UV-Visible absorption titration in the range of 200-500 nm. The quenching interactions of metal complexes with BSA were monitored by change in their fluorescence intensities at a fixed excitation wave length of 285 nm and emission value at 345 nm, respectively. The same emission and excitation scan rates and slit widths were maintained throughout the experiments. Fixed protein concentration (1 μM) was used to titrate against different concentrations of the metal complexes (0-24 μM).

The CD spectral studies were also carried out with ct-DNA (100 μM) and BSA (10 μM) with varying concentrations of metal complexes (0-12 μM) in the range of 200-300 nm, using buffer alone as a blank control. All the solutions for ct-DNA and protein studies were prepared in 5 mM Tris-HCl buffer (pH-7.2) and phosphate buffer (pH-7.2), respectively. Each experiment was performed in triplicates and the average value was taken to minimize the signal to noise ratio.

2.8 Computational studies to reveal the nature of interaction of copper complexes with DNA and protein

2.8.1 Receptor and Ligand preparation

The interactions of the four copper complexes **1-4** towards the DNA and BSA (protein) were studied using molecular docking analysis. The X-ray crystal structures of Bovine

serum albumin protein in complex with 3, 5-diiodosalicylic acid (PDB ID: 4JK4) and ct-DNA (PDB ID: 355D) obtained from Brookhaven Protein Data Bank were considered for docking studies [34, 35]. The crystal structures were refined by removing the water molecules and hetero atoms. Hydrogen atoms were added to the protein and ct-DNA molecule. The kollman charges [36] were assigned to the protein atoms using Auto DockTools-1.5.6. The 3D coordinates of the synthesized complexes **1-4** were built and optimized using molecular mechanics. Gasteiger partial atomic charges [37] were added to the optimized complexes and ct-DNA. The possible flexibility and torsion of the complexes were defined by using Auto Tors. The copper metal complexes were treated to be flexible using AutoDock 4.2. The most active binding site for **3**, was identified [35] by defining a grid box around the active site. In case of ct-DNA, a blind docking was performed by covering the entire DNA to identify the binding site. Grid maps of interaction energies between protein/DNA and various types of atoms present in the complexes were pre-calculated using Auto Grid program.

2.8.2 Docking studies

Docking calculations were performed with default parameters implemented in AutoDock 4.2 [38]. It evaluates the conformational changes obtained after the binding of ligand to the receptor and also their structural integrity. Scoring functions elucidate the intermolecular energy difference between the bound and unbound states of the protein. It also calculates the intermolecular energy due to receptor-ligand interactions. Prior to docking, the geometries of the complexes were optimized with LANL2DZ, 6–31+G** and 6–31G* basis and a B3LYP functional in Gaussian 09 program. The probable bound conformations and the energies of the flexible complexes were explored using Lamarckian genetic algorithm (LGA) and AMBER force field, respectively. The binding energy was evaluated using the following scoring function:

$$\Delta G = \Delta G_{vdw} + \Delta G_{hbond} + \Delta G_{elec} + \Delta G_{tor} + \Delta G_{desolv}$$

The free energy upon binding of the flexible ligand to the rigid target can be calculated using the equation that includes parameters like ΔG_{vdw} (dispersion/repulsion), ΔG_{elec}

(electrostatic interaction), ΔG_{hbond} (hydrogen bonding), ΔG_{tor} (torsional constraints) and ΔG_{sol} (desolvation effects).

2.9 Evolution of cytotoxicity by MTT assay

Cytotoxic studies of copper(II) complexes (**1-4**) were carried out on human liver carcinoma cell line (HepG-2), procured from the American Type Culture Collection (ATCC HB-8065), USA. The viability of cells was screened by MTT assay [39]. The obtained cells were cultured in a sterile T75 flask containing Dulbecco's Modified Eagle's medium (DMEM) supplemented with fetal bovine serum (10% v/v) at 37 °C in an incubator with humidified atmosphere of 95% air and 5% CO_2.

The complexes were dissolved in 5 mM phosphate buffered saline (PBS, pH 7.2) containing 10% DMSO. Concentration of the DMSO was maintained below 0.5% for cell survival. The HepG-2 cells were plated separately in 96 well plates at a concentration of 1×10^5 cells/well. After 24h, the cells were washed twice with 100 µl of serum-free medium and starved for an hour at 37 °C. After starvation, the cells were treated with different concentrations of complexes (50-150 µg/ml) for 24h. At the end of the treatment period, the medium was aspirated and serum free medium containing MTT (0.5 mg/ml) was added and incubated for 4h at 37 °C in a CO_2 incubator. The MTT containing medium was then discarded and the cells were washed with PBS (200 µl). Only the live cells can take in MTT and convert it in to formazan crystals. Afterwards, the cells were lysed by adding DMSO and further dissolved formazan imparted purple blue colour to the buffer solution. This conversion was monitored by change in absorbance at 579 nm in a micro titer plate reader (Biorad 680). Cytotoxicity was determined using Microsoft excel. The percentage of cell viability was calculated using the formula;

$$\% \text{ viability} = \{\text{OD of the experiment samples/OD of the control}\} \times 100$$

3. Results and Discussion

3.1 Synthesis

2.0 Moles of 2-acetyl pyridine and 1.0 mole of 2-pyridinecarboxaldehyde were used for the preparation of 4′-(2‴-Pyridyl)-2, 2′:6′, 2″-terpyridine ligand in presence of KOH as a base (Scheme 1) and the ligand structure was confirmed by spectroscopic techniques. Copper(II) nitrate tri hydrate [Cu $(NO_3)_2.3H_2O$] was used as precursor for the synthesis of new copper(II) derivatives (Scheme 2). All the newly synthesized metal complexes were characterized by elemental analysis and various spectroscopic techniques. The molecular structure of copper complex **2** was confirmed by single crystal X-ray diffraction studies.

3.2 Characterization

The electronic absorption spectra of ligand (2‴-pytpy) and its metal complexes (**1-4**) show intense bands in the range of 200-400 nm (Fig. S1, ESI†). All the new copper(II) complexes exhibit four bands. The bands at 242 and 280 nm can be assigned to n-π* and π-π* transitions of aromatic rings. The bands appearing in the range of 252-288 nm correspond to the intra-ligand transitions (π-π*, n-π*) of 4′-(2‴-Pyridyl)-2, 2′:6′, 2″-terpyridine ligand. The bands appearing at ~334 nm and ~ 349 nm, corresponds to the ligand to metal charge transfer band (LMCT). The weak d-d transitions which are supposed to be in the visible region (~600 nm) of the spectrum were not observed for copper(II) complexes due to the dominant tail arising from the charge transfer transition [40, 41].

The FT-IR spectrum of 4′-(2‴-Pyridyl)-2, 2′:6′, 2″-terpyridine shows strong band at 1581 cm^{-1} which corresponds to the C=N stretching (Fig. S2, ESI†). In case of complexes (**1-4**), the medium C=N stretch band is shifted towards higher values and are observed in the range of 1604-1616 cm^{-1} (Fig. S3-S6, ESI†). This indicates the binding of nitrogen atom to copper metal is through coordination fashion. The uncoordinated ancillary ligands show the same medium C=N stretching band in the frequency range of 1579-1589 cm^{-1}. In all complexes a strong intense band at 1384 cm^{-1} confirms the presence of nitrate as counter ion. The stretching band corresponding to the coordinated water molecule was found between 783-785 cm^{-1}.

4′-(2‴-Pyridyl)-2, 2′:6′, 2″-terpyridine structure was confirmed by both NMR and mass spectrometry techniques (Fig. S7-S9, ESI†). The ^{1}H NMR spectrum of the ligand shows expected chemical shift values for aromatic protons in the region of 7.26 - 9.10 δ ppm and ^{13}C NMR spectrum reveals chemical shift values for all identical carbon entities of the ligand in the range of 118.63 - 156.25 δ ppm. The molecular weight of the ligand was confirmed by ESI mass spectroscopy. The molecular ion peak M+1 was observed at 311.40 *m/z* (310.12). The molecular mass of all the synthesized complexes were confirmed by LC-MS (Fig. S10-S13, ESI†). Complexes **1** and **4** show M+2 peaks at 531 (529.12), 657 (655.14) and complex **2**, **3** display molecular ion peak (M+1) at 554 (553.12) and 606 (605.13), respectively.

3.3 Crystal Structure

Single crystal X-ray diffraction analysis was carried out for the extensive structural characterization of complex **2**. The perspective view of the complex, ORTEP diagram is given in Fig. 1. A keen investigation on the structure revealed that it belongs to the *P*1 space group of the triclinic system and detailed crystallographic data of complex **2** is summarized in Table S1†. The penta-coordinated crystal structure of complex **2** exhibited a distorted square-pyramidal geometrical (Cu-N_5) system in tridentate and bidentate binding fashion from 4′-(2‴-Pyridyl)-2, 2′:6′, 2″-terpyridine (2‴-pytpy) ligand and the phenanthroline base, respectively. The 2‴-pytpy ligand binds to the bansal plane of the complex **2** and an axial-equatorial mode of binding was observed with the phenanthroline base. In the bansal plane of 2‴-pytpy ligand, nitrogen {N(2)} is positioned at a distance of 1.932 Å and the axial position of phenanthroline base nitrogen {N(5)} was at a bond distance of 2.278 Å from the central copper ion. The other three nitrogen's {N (1), N (3) and N (4)} are linked with central metal ion at a distance of 2.055 Å, 2.060 Å and 1.999 Å, respectively. Selected bond distances and bond angles are tabulated in Table S2†.

3.4 Computation methods

The optimized structures of copper(II) complexes (**1-4**) are depicted in Fig. S14, ESI†. Calculated and experimental geometrical parameters of all the derivatives are shown in Table 1. The results reveal that all the calculated geometrical parameters are in good agreement with the experimental values except for the bond length of Cu–N (the difference

in the bond length is ~ 0.50 Å). The reason for this deviation could be due to constraints arising from the crystal packing arrangement. The theoretically optimized geometry data were compared with the crystallographic data and the validation of the method was authenticated from the structural similarity observed between both the methods. Further, similar computational procedures were employed for other complexes **1**, **3** and **4** for which crystal structure data are not available. The calculated geometrical parameters of the complexes (**1**, **3** and **4**) are also given in Table 1 along with the calculated electronic transition bands of the complexes (**1-4**) (Table S3†). Theoretical absorption peaks of all the complexes were compared with the experimental (electronic absorption) values. All the theoretical and experimental absorption values are found to be in good agreement. The molecular orbitals (Fig. 2) involved in the transitions and their major contributions for the transitions are tabulated in Table S3† (Fig. S15, ESI†). Theoretical and experimental values are supporting each other in the frame work of TD-DFT.

3.5.1 UV-Visible absorption titration

UV-Visible absorption spectroscopy was used to calculate the binding propensity of metal complexes with ct-DNA. Metal complexes (20 µM) were titrated with varying concentrations of ct-DNA (0-26 µM) and is depicted in Fig. 3. The increasing concentration of ct-DNA to metal complexes shows a significant hypochromism (48.71-67.19 %) with small red shift (~1 nm) due to the strong stacking interaction between the DNA base pairs and aromatic chromophore of the ligands [42]. The results indicate that complexes bind to ct-DNA *via* intercalative mode. The intrinsic binding constant (K_b) values of complexes with ct-DNA were calculated using the following equation:

$$[DNA]/ (\varepsilon_a - \varepsilon_f) = [DNA]/ (\varepsilon_b - \varepsilon_f) + 1/ K_b (\varepsilon_b - \varepsilon_f)$$

Here [DNA] is the concentration of the DNA in base pairs, the apparent absorption coefficients ε_a, ε_f and ε_b correspond to A_{obsd} / [complex], extinction coefficient for complex in free form and extinction coefficient for DNA bound complex, respectively. The intrinsic binding constant (K_b) is obtained from the ratio of slope to intercept [43]. The binding constant values (K_b) of metal complexes (**1-4**) were found to be in the range of 2.75×10^5 to 7.85×10^5 M^{-1}. The mode of binding of the metal complexes with DNA might have been

influenced by the planarity of 4′-(2‴-Pyridyl)-2, 2′:6′, 2″-terpyridine and ancillary ligands (bpy, phen, dpq and dppz). The dpq and dppz containing complexes (**3** & **4**) show high binding constants when compared with bpy and phen containing metal complexes (**1** & **2**) which could be due to the extended aromatic moiety [44].

3.5.2 Competitive binding interaction between Ethidium Bromide (EtBr) and metal complexes with ct-DNA

Neither metal complexes nor the ct-DNA displayed intrinsic fluorescence emission either alone or in combination. Therefore, the binding interaction of complexes with ct-DNA could not be identified directly through fluorescence emission. A competitive binding experiment was carried out to evaluate the mode of interaction, wherein EtBr was not only used as a fluorescent probe but also to compete with the binding of ct-DNA to the metal complexes. EtBr a planar cationic dye with phenanthridine ring is used as a fluorescence probe for native DNA. The intense fluorescence emission observed from EtBr in the presence of ct-DNA is due to strong interaction between adjacent DNA base pairs via intercalative binding [45]. The remarkable decrease in fluorescence intensity of EtBr-ct-DNA with increasing concentration (0-20 µM) of quencher is shown in Fig. 4. The emission band at 598 nm displayed hypochromism up to 79.50 %, 85.71 %, 85.83 % and 87.80 % of the initial fluorescence intensity for **1-4**, respectively. The EtBr bound ct-DNA enhanced fluorescence intensity values were quenched by metal complexes due to its replacement for EtBr in ct-DNA: EtBr complex. The quenching constants of metal complexes were analyzed by following Stern-Volmer equation:

$$I_0 / I = 1 + K_{sv}\,[Q]$$

Here I_0 and I are the emission intensities in the absence and presence of quencher, respectively. K_{sv} is the linear Stern-Volmer quenching constant, and [Q] is the concentration of quencher. The K_{sv} value was obtained from slope of I_0 / I vs. [Q]. The quenching plot depicts that the quenching of EtBr bound to ct-DNA by metal complexes are in good agreement with the Stern-Volmer equation. The quenching constant values (K_{sv}) for complexes (**1-4**) were found to be 1.023×10^5 M^{-1}, 1.09×10^5 M^{-1}, 1.183×10^5 M^{-1} and

1.264×10^5 M^{-1}, respectively. The apparent binding constant (K_{app}) values for metal complexes were obtained from the following equation:

K_{EB} [EB] = K_{app} [complex]

Here K_{EB} = 1.0×10^7 M^{-1}, [EB] = 5 μM and [complex] is the complex concentration at 50 % reduction in the fluorescence intensity of EB. The quenching constant K_{app} values of metal complexes (**1-4**) are found to be 5.11×10^6 M^{-1}, 5.45×10^6 M^{-1}, 5.91×10^6 M^{-1} and 6.37×10^6 M^{-1}, respectively. These results suggest that all the metal complexes bind with ct-DNA *via* intercalation mode and binding constant values are less while comparing with other classical intercalators [46].

3.5.3 In-silico analysis

In chemotherapy treatments, the biological processes inside the cell are influenced by the structure and conformations of protein / DNA while binding partners interact. In order to establish this, docking calculations were performed to observe the interaction and binding affinity of all the four copper(II) complexes with ct-DNA and BSA protein (Fig. 5 and Fig. 6). In case of ct-DNA, initially a blind docking was executed to identify the binding pockets. Similar procedure was then repeated with grid boxes covering only the major and minor grooves independently. The binding (ΔG_{BE}) and intermolecular energies ($\Delta G_{intermol}$) of the complexes **1-4** with ct-DNA and protein are given in Table 2 and Table 3, respectively. Docking calculations of complexes **1-4** with ct-DNA revealed similar binding energies (~ −10.00 kcal/mol). The interaction for complexes **1-3** mainly depends upon hydrogen bonding. The pyrimidine (C_{21} OP_1) of complexes **1, 2** and **3** formed hydrogen bonds with the nitrogen atom of terpyridine ring. ct-DNA docking studies revealed that the complexes **1-4** interact with ct-DNA *via* major groove with high binding affinities. The interactions reveal that the complexes **1-4** can serve as potent therapeutic candidates and chemotherapeutic agents for the treatment of cancers.

Molecular docking was also carried out to investigate the protein-ligand interactions and hence to display all structural features of the protein and the stereo-chemical properties of all the binding complexes. In this study the interaction of the four synthesized copper(II)

complexes were analyzed for their binding affinity and their interactions towards the BSA protein. Fig. 6 depicts the residues involved in the interaction with copper complexes **1-4** and their binding energy, torsional energy, intermolecular, electrostatic energy for each protein–complex are provided in Table 3.

In case of Bovine serum albumin binding studies, the interaction of complex **4** is predominantly stabilized by hydrophobic interactions with the residues Lys116, Pro117, Leu178, Arg185, Thr514 and Pro516. The intermolecular energy contribution of the complex **4** to the total energy was ~ −6.00 kcal/mol for BSA protein and the contribution of complex **1-4** to the total energy was ~ −11.00 kcal/mol for ct-DNA. This shows that there exists a strong intermolecular van der Waals, hydrogen bonding, desolvation and electrostatic interactions. The best docked conformation of complexes with ct-DNA and BSA obtained by docking calculations is exhibited in Fig. 5 and Fig. 6, respectively. Based on docking calculations, it is observed that complex **4** shows better binding affinity with BSA compared to other complexes. These results are agree well with the experimental data.

3.6 BSA interaction studies

In order to study the nature of interaction between BSA and the metal complexes, electronic spectrum was recorded by titrating a fixed amount of protein against varying concentration of metal complexes (**1-4**). Quenching effect was observed with (Fig .7). The decrease in the emission intensity of BSA with metal complexes indicates the type of interaction between protein and metal complex and induces static quenching rather than dynamic quenching as a shift in the absorption spectra was not observed [47].

Mainly the presence of amino acids phenylalanine, tyrosine and tryptophan are responsible for the fluorescence of BSA [48-50]. Out of these three, tryptophan plays a major role in the intrinsic fluorescence of BSA. Fluorescence spectral titrations were carried out in the wave length range of 285-500 nm upon excitation at 280 nm. The effect of copper(II) complexes on fluorescence spectra of protein is given in Fig. 7. The increasing concentration of metal complexes (0 - 24 µM) shows a significant quenching of fluorescence intensity at 345 nm, up to 84.07 %, 89.78 %, 93.07 % and 82.56 %, respectively of the initial fluorescence intensity of BSA accompanied by a hypsochromic

shift of ~ 2 - 4 nm for the metal complexes (**1-4**). The blue shift observed is mainly due to the binding of metal complexes with the active site of protein in a hydrophobic environment.

The fluorescence quenching constant values are described by the Stern-Volmer equation

$I_0 / I = 1 + K_{sv}$ [Q]

Here I_0 and I indicate the fluorescence intensities in the absence and presence of metal complex (quencher), respectively. K_{sv} is a linear Stern-Volmer quenching constant, and [Q] is the quencher concentration. The quenching constant (K_q) can be calculated using the plot of log (I_0 / I) *versus* log [Q].

If small molecules bind independently to a set of equivalent sites on a macromolecule, the equilibrium between free and bound molecules is represented by the Scatchard equation: [5, 52]

$\log [(I_0 - I)/ I] = \log K_b + n \log [Q]$

Here K_b is the binding constant of the complex with BSA and n is the number of binding sites. Employing the plot of log [(I_0- I)/ I] *versus* log [Q], the number of binding sites (n) and the binding constant (K_b) values could be obtained. The quenching constant (K_q), binding constant (K_b) and number of binding sites (n) for the interaction of the Cu(II) complexes with BSA are shown in Table 4. The results indicate that in all the complexes, only one binding site is available for interaction with BSA.

*3.7 Circular Dichroism spectral analysis of metal complexes (**1-4**) with ct-DNA and BSA*

Circular Dichroism spectral analysis was carried out to investigate conformational changes induced in the secondary structure of ct-DNA by the metal complexes [53]. The characteristic CD spectrum of ct-DNA in its right handed B-form, exhibits a positive band at 275 nm and a negative band at 245 nm corresponding to π-π base stacking and helical structure, respectively [54]. The interaction studies revealed a slight increase in the intensity of negative band and a slight decrease in intensity of positive band with a blue shift of 10 – 17 nm and 2 – 11 nm, respectively with hypsochromic shift for all the complexes as

provided in Fig. 8. Surprisingly, in case of complexes **2-4** with increase in concentrations (0-12 μM), there is a huge blue shift in the long wave length band from 275 nm to ~269 nm. These results suggest that complexes bind with DNA *via* intercalative mode with strong conformational changes at higher concentrations of metal complexes [55, 56].

The conformational change caused by the metal complexes upon binding with protein is also investigated from the CD spectra. Metal complexes may affect the secondary or tertiary structure of proteins. The typical CD spectrum of BSA shows two negative bands at 208 nm and 222 nm. The red shift observed in the band around 222 nm corresponds to the n-π* transition from the peptide bond of α-helix [57, 58]. Fig. 9 reveals the influence of copper(II) complexes (**1-4**) on the secondary structure of the protein. At lower concentration of metal complexes, there is a slight increase in right handed helical content of BSA. These results suggest that there is a conformational change in the secondary structure of protein in the presence of metal complexes.

3.8 In vitro cytotoxicity studies

MTT assay was followed to assess the influence of complexes (**1-4**) on the percentage cell viability of HepG-2 cell lines. From the cell viability (%) *vs* complex concentration plot (Fig. 10), a dose dependent activity was observed towards HepG-2 cell lines. The half maximal inhibitory concentration (IC_{50}) values of complexes **1-4** were found to be 76.9, 51.4, 39.2 and 23.8 μg/ml, respectively. Among the four metal complexes, **4** exhibits better cytotoxicity towards the HepG-2 cell line.

4. Conclusion

Herein, new copper(II) heteroleptic mononuclear complexes were synthesized, structurally characterized and assessed for their biological activities. The single crystal X-ray diffraction studies of complex **2** reveals a penta-coordination around copper ion with distorted square-pyramidal geometry. An intercalative binding mode of metal complexes with DNA was observed when their binding properties with DNA were getting examined by UV-Visible absorption, fluorescence and CD spectral titrations. The binding efficacy of

DNA with complexes follows the order **1 < 2 < 3 < 4**. The interaction of complexes with protein was revealed from the observation of static quenching in electronic spectrum of BSA. In addition, in vitro cytotoxicity of copper(II) complexes against HepG-2 cell lines provides satisfactory IC_{50} values. Thus, based on the above investigations followed by description, it could be concluded that these new copper(II) complexes enrich the library of potent anticancer drugs and could open up avenues for further exploringtheir applications towards next level of biological studies such as genomic and topoisomerase activities.

Acknowledgement

Authors extend their heartfelt thanks to the VIT University, Vellore, India for expediting essential requirements and financial support. Author T.K. gratefully acknowledge administration of VIT University for awarding him research associateship.

References

[1] Y. Kidani, Development of antitumor platinum complexes, Jpn. J. Cancer Chemother. 10 (1983) 2442-2452.

[2] B. Rosenberg, Platinum coordination complexes in cancer chemotherapy, Naturwissenschaften. 60 (1973) 399-406.

[3] R. J. Speer, H. Ridgway, L. M. Hall, D. P. Stewart, K. E. Howe, D. Z. Lieberman, A. D. Newman, J. M. Hill, Coordination complexes of platinum as antitumor agents, Cancer Chemother. Rep. 59 (1974) 629-641.

[4] B. Drewinko, L. Y. Yang, Ligands of second generation platinum analogs decrease both platinum-induced DNA cross-linking and its ability to interact with 1-β-D-arabinofuranosyl cytosine to potentiate cytotoxic efficacy, Chem.-Biol. Interact. 60 (1986) 159-169.

[5] P. C. Hydes, M. J. Russell, Advances in platinum cancer chemotherapy, Cancer Metastasis Rev. 7 (1988) 67-89.

[6] X. Sun, C. N. Tsang, H. Sun, Identification and characterization of metallo-drug binding proteins by (metallo) proteomics, Metallomics. 1 (2009) 25-31.

[7] Q. He, C. H. Liang, S. J. Lippard, Steroid hormones induce HMG1 overexpression and sensitize breast cancer cells to cisplatin and carboplatin, Proceedings of the National Academy of Sciences, Proc. Natl. Acad. Sci. U. S. A. 97 (2000) 5768-5772.

[8] D. B. Zamble, Y. Mikata, C. H. Eng, K. E. Sandman, S. J. Lippard, Testis-specific HMG-domain protein alters the responses of cells to cisplatin, J. Inorg. Biochem. 91 (2002) 451-462.

[9] A. W. Prestayko, J. C. D'Aoust, B. F. Issell, S. T. Crooke, Cisplatin (cis-diammine dichloroplatinum II), Cancer Treat. Rev. 6 (1979) 17-39.

[10] M. Galanski, M. A. Jakupec, B. K. Keppler, Update of the preclinical situation of anticancer platinum complexes: novel design strategies and innovative analytical approaches, Curr. Med. Chem. 12 (2005) 2075-2094.

[11] D. Wang, S. J. Lippard, Cellular processing of platinum anticancer drugs, Nat. Rev. Drug Discovery. 4 (2005) 307-320.

[12] E. L. M. Wong, G. S. Fang, C. M. Che, N. Zhu, Highly cytotoxic iron (II) complexes with Penta dentate pyridyl ligands as a new class of anti-tumor agents, Chem. Commun. 36 (2005) 4578-4580.

[13] A. Terenzi, M. Fanelli, G. Ambrosi, S. Amatori, V. Fusi, L. Giorgi, V. T. Liveria, G. Barone, DNA binding and antiproliferative activity toward human carcinoma cells of copper (II) and zinc (II) complexes of a 2, 5-diphenyl [1, 3, 4] oxadiazole derivative, Dalton Trans. 41 (2012) 4389-4395.

[14] J. Osredkar, N. Sustar, Copper and zinc, biological role and significance of copper/zinc imbalance, Journal of Clinical Toxicology, J. Clin. Toxicol. (2011) DOI: 4172/2161-0495.S3-001, S: 3, 1.

[15] E. D. Harris, Copper homeostasis: the role of cellular transporters, Nutr. Rev. 59 (2001) 281-285.

[16] S. J. Lippard, J. M. Berg, Principles of bioinorganic chemistry, University Science Books, Mill Valley, CA, 1994.

[17] X. Cao, S. V. Antonyuk, S. V. Seetharaman, L. J. Whitson, B. Taylor, S. P. Holloway, R. W. Strange, P. A. Doucette, J. S. Valentine, A. Tiwari, L. J. Hayward, S. Padua, J. A. Cohlberg, S. S. Hasnain, P. J. Hart, Structures of the G85R variant of SOD1 in familial amyotrophic lateral sclerosis, J. Biol. Chem. 23 (2008) 16169-16177.

[18] L. Leinartaite, K. Saraboji, A. Nordlund, D. T. Logan, M. Oliveberg, Folding catalysis by transient coordination of Zn^{2+} to the Cu ligands of the ALS-associated enzyme Cu/Zn superoxide dismutase 1, J. Am. Chem. Soc. 132 (2010) 13495-13504.

[19] V. M. Manikandamathavan, B. U. Nair, DNA binding and cytotoxicity of copper (II) imidazole terpyridine complexes: Role of oxyanion, hydrogen bonding and π–π interaction, Eur. J. Med. Chem. 68 (2013) 244-252.

[20] V. M. Manikandamathavan, V. Rajapandian, A. J. Freddy, T. Weyhermuller, V. Subramanian, B. U. Nair, Effect of coordinated ligands on antiproliferative activity and DNA cleavage property of three mononuclear Cu (II)-terpyridine complexes, Eur. J. Med. Chem. 57 (2012) 449-458.

[21] G. Sathyaraj, T. Weyhermuller, B. U. Nair, Synthesis, characterization and DNA binding studies of new ruthenium (II) bis terpyridine complexes, Eur. J. Med. Chem., 45 (2010) 284-291.

[22] V. G. Vaidyanathan, B. U. Nair, Synthesis, characterization and binding studies of chromium (III) complex containing an intercalating ligand with DNA, J. Inorg. Biochem. 95 (2003) 334-342.

[23] R. Vijayalakshmi, M. Kanthimathi, V. Subramanian, B. U. Nair, Interaction of DNA with [Cr (Schiff base) $(H_2O)_2$] ClO_4, Biochim. Biophys. Acta. 1475 (2000) 157-162.

[24] V. M. Manikandamathavan, T. Weyhermuller, R.P. Parameswari, M. Sathish kumar, V. Subramanian, B. U. Nair, DNA/Protein interaction and cytotoxic activity of Imidazole terpyridine derived Cu (II)/Zn (II) metal complexes, Dalton Trans., 43, (2014) 13018-13031.

[25] V. Uma, M. Kanthimathi, T. Weyhermuller, B. U. Nair, Oxidative DNA cleavage mediated by a new copper (II) terpyridine complex: crystal structure and DNA binding studies, J. Inorg. Biochem.99 (2005) 2299-2307.

[26] W. Paw, R. Eisenberg, Synthesis, characterization, and spectroscopy of dipyrido catecholate complexes of platinum, Inorg. Chem. 36 (1997) 2287-2293.

[27] M.N. Patel, H.N. Joshi, C.R. Patel, DNA interaction, in vitro antimicrobial and SOD-like activity of copper (II) complexes with norfloxacin and terpyridines, J. Organomet. Chem. 701 (2012) 8-16.

[28] G. M. Sheldrick, A short history of SHELX, Acta Crystallogr. Sect. A., 64 (2007) 112-122.

[29] G.W.T. M.J. Frisch, H.B. Schlegel, G.E. Scuseria, M.A. Robb, J.R. Cheeseman, G. Scalmani, V. Barone, B. Mennucci, G.A. Petersson, H. Nakatsuji, M. Caricato, X. Li, H.P. Hratchian, A.F. Izmaylov, J. Bloino, G. Zheng, J.L. Sonnenberg, M. Hada, M. Ehara, K. Toyota, R. Fukuda, J. Hasegawa, M. Ishida, T. Nakajima, Y. Honda, O. Kitao, H. Nakai, T. Vreven, J.A. Jr. Montgomery, J.E. Peralta, F. Ogliaro, M. Bearpark, J.J. Heyd, E. Brothers, K.N. Kudin, V.N. Staroverov, R. Kobayashi, J. Normand, K. Raghavachari, A. Rendell, J.C. Burant, S.S. Iyengar, J. Tomasi, M. Cossi, N. Rega, J.M. Millam, M. Klene, J.E. Knox, J.B. Cross, V. Bakken, C. Adamo, J. Jaramillo, R. Gomperts, R.E. Stratmann, O. Yazyev, A.J. Austin, R. Cammi, C. Pomelli, J.W. Ochterski, R.L. Martin, K. Morokuma, V.G. Zakrzewski, G.A. Voth, P. Salvador, J.J. Dannenberg, S. Dapprich, A.D. Daniels, O. Farkas, J.B. Foresman,

J.V. Ortiz, J. Cioslowski, D.J. Fox, C.T. Wallingford, Gaussian 09, in, Gaussian Inc, 2009.

[30] C.W. Hsu, C.C. Lin, M.W. Chung, Y. Chi, G.H. Lee, P.T. Chou, C.H. Chang, P.Y. Chen, Systematic Investigation of the Metal-Structure–Photophysics Relationship of Emissive d10-Complexes of Group 11 Elements: The Prospect of Application in Organic Light Emitting Devices, J. Am. Chem. Soc. 133 (2011) 12085-12099.

[31] F. De Angelis, S. Fantacci, A. Sgamellotti, E. Cariati, R. Ugo, P.C. Ford, Electronic transitions involved in the absorption spectrum and dual luminescence of tetra nuclear cubane [Cu_4I_4 (pyridine) $_4$] cluster: a density functional theory/time-dependent density functional theory investigation, Inorg. Chem. 45 (2006) 10576-10584.

[32] V. Uma, M. Elango, B.U. Nair, Copper (II) terpyridine complexes: effect of substituent on DNA binding and nuclease activity, Eur. J. Inorg. Chem. 22 (2007) 3484-3490.

[33] M.E. Reichmann, S.A. Rice, C.A. Thomas, P. Doty, A further examination of the molecular weight and size of desoxypentose nucleic acid, J. Am. Chem. Soc. 76 (1954) 3047-3053.

[34] B. Sekula, K. Zielinski, A. Bujacz, Crystallographic studies of the complexes of bovine and equine serum albumin with 3, 5-diiodosalicylic acid, Int J Biol Macromol. 60 (2013) 316-324.

[35] K. Suntharalingam, O.Mendoza, A.A. Durate, D.J. Mann, R.Vilar, A platinum complex that binds non-covalently to DNA and induces cell death via a different mechanism than cisplatin, Metallomics. 5 (2013) 514-523.

[36] U. C. Singh, P. A. Kollman, An approach to computing electrostatic charges for molecules, J. Comput. Chem. 5 (1984) 129-145.

[37] J. Gasteiger, M.Marsili, Iterative partial equalization of orbital electronegativity-a rapid access to atomic charges, Tetrahedron. 36 (1980) 3219-3228.

[38] G. M. Morris, D. S. Goodsell, R.S. Halliday, R. Huey, W. E. Hart, R. K. Belew, A. J. Olson, Automated docking using a Lamarckian genetic algorithm and an empirical binding free energy function, J. Comput. Chem. 19 (1998) 1639-1662.

[39] T. Mossman, Rapid colorimetric assay for cellular growth and survival: application to proliferation and cytotoxicity assays, J. Immunol. Methods.65 (1983) 55-63.

[40] C. Gokce, R. Gup, Copper (II) complexes of acylhydrazones: synthesis, characterization and DNA interaction, Appl. Organometall. Chem., 27 (2013) 263-268.

[41] C. Gokce, R. Gup, Synthesis, characterization and DNA interaction of new copper (II) complexes of Schiff base-aroylhydrazones bearing naphthalene ring, J. Photochem. Photobiol. B: Biol. 122 (2013) 15-23.

[42] J .S.Guerrero, P.C. Sanchez, E.R. Perez, F.V. Garcia, M.E.B.Gomez, L. R. Azuara, Genotoxicity of the copper antineoplastic coordination complexes casiopeinas®, Toxicology in Vitro. 25 (2011) 1376-1384.

[43] P.R. Reddy, A. Shilpa, N. Raju, P. Raghavaiah, Synthesis, structure, DNA binding and cleavage properties of ternary amino acid Schiff base-phen/bipy Cu (II) complexes, J. Inorg. Biochem. 105 (2011) 1603-1612.

[44] P.K. Sasmal, R. Majumdar, R.R. Dighe, A.R. Chakravarty, Photocytotoxicity and DNA cleavage activity of L-arg and L-lys Schiff base oxovanadium (IV) complexes having phenanthroline bases, Dalton Trans. 39 (2010) 7104-7113.

[45] D. Senthil Raja, S.P. Nattamai, K.N. Bhuvanesh, Synthesis, crystal structure and pharmacological evaluation of two new Cu (II) complexes of 2-oxo-1, 2-dihydroquinoline-3-carbaldehyde (benzoyl) hydrazone: A comparative investigation, Eur. J. Med. Chem. 47 (2012) 73-85.

[46] M. Cory, D.D. McKee, J. Kagan, D.W. Henry, J.A. Miller, Design, synthesis, and DNA binding properties of bifunctional intercalators. Comparison of polymethylene and diphenyl ether chains connecting phenanthridine, J. Am. Chem. Soc., 107 (1985) 2528-2536.

[47] D. Senthil Raja, G. Paramaguru, N. S. P. Bhuvanesh, J. H. Reibenspies, R. Renganathan, K. Natarajan, Effect of terminal N-substitution in 2-oxo-1, 2-dihydroquinoline-3-carbaldehyde thiosemicarbazones on the mode of coordination, structure, interaction with protein, radical scavenging and cytotoxic activity of copper (II) complexes, Dalton Trans. 40 (2011) 4548-4559.

[48] K. A. Z. Osama, I. K. A. S. H. Othman,). Characterization of subdomain IIA binding site of human serum albumin in its native, unfolded, and refolded states using small molecular probes, J. Am. Chem. Soc. 130 (2008) 10793-10801.

[49] G. Sudlow, D. J. Birkett, D. N. Wade, Further characterization of specific drug binding sites on human serum albumin, Mol. Pharmacol. 12 (1976) 1052-1061.

[50] S. Wanwimolruk, D. J. Birkett, P. M. Brooks, Structural requirements for drug binding to site II on human serum albumin, Mol. Pharmacol. 24 (1983) 458-463.

[51] J. R. Lakowicz, Fluorescence Quenching: Theory and Applications. Principles of Fluorescence Spectroscopy, Kluwer Academic/Plenum Publishers, New York, 1999.

[52] X. Z. Feng, Z. Yang, L. J. Wang, C. Bai, Investigation of the interaction between acridine orange and bovine serum albumin, Talanta. 47 (1998) 1223-1229.

[53] A.M. Polyanichko, V.V. Andrushchenko, E.V. Chikhirzhina, V. Vorobev, H. Wieser, The effect of manganese (II) on DNA structure: electronic and vibrational circular dichroism studies, Nucleic Acids Res. 32 (2004) 989-996.

[54] V.I. Ivanov, L.E. Minchenkova, A.K. Schyolkina, A.I. Poletayer, Different conformations of double-stranded nucleic acid in solution as revealed by circular dichroism, Biopolymers. 12 (1973) 89-110.

[55] O. Novakova, H. Chen, O. Vrana, A. Rodger, P. J. Sadler, V. Brabec, DNA interactions of monofunctional organometallic ruthenium (II) antitumor complexes in cell-free media, Biochemistry. 42 (2003) 11544-11554.

[56] B. Norden, F. Tjerneld, Structure of methylene blue–DNA complexes studied by linear and circular dichroism spectroscopy, Biopolymers. 21 (1982) 1713-1734.

[57] J. Q. Liu, J. N. Tian, X. Tian, Interaction of isofraxidin with human serum albumin, Bioorg. Med. Chem. 12 (2004) 469-474.

[58] B. Ranjbar, P. Gill, Circular Dichroism Techniques: Biomolecular and Nano structural Analyses-A Review, Chem. Biol. Drug Des. 74 (2009) 101-120.

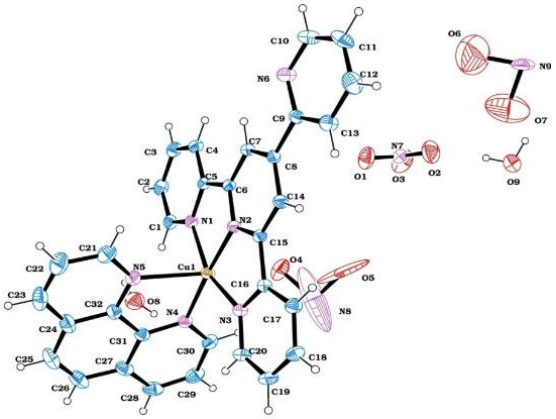

Fig. 1. ORTEP diagram of complex **2** (CCDC: 1431231).

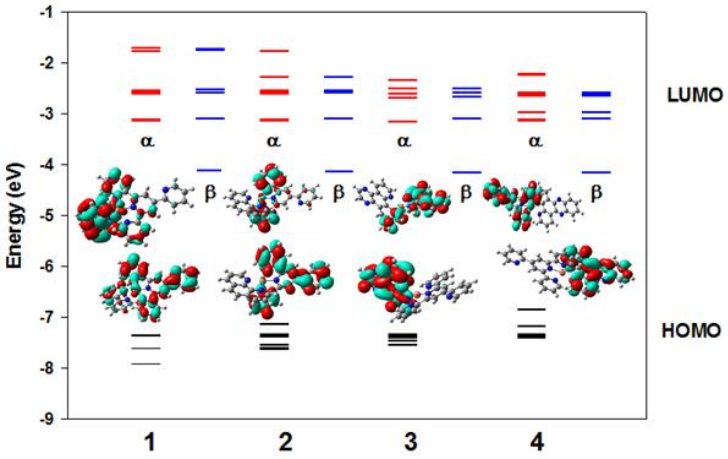

Fig. 2. Contour plots of HOMOs and LUMOs with the orbital energies of complex **1-4**.

3.5 DNA interaction studies

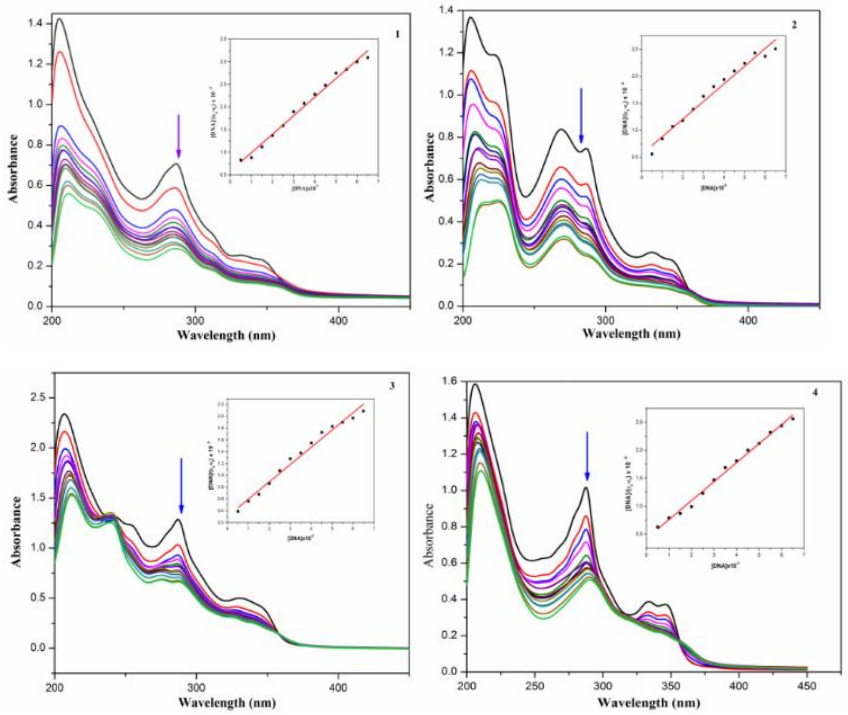

Fig. 3. Electronic absorption spectra depicting the titration of complexes **1-4** vs DNA. The arrows indicate the decrease in the absorbance with increasing concentration of DNA concentration (0 – 26 μM). The intrinsic binding constant can be calculated from the intercept of the inset graph.

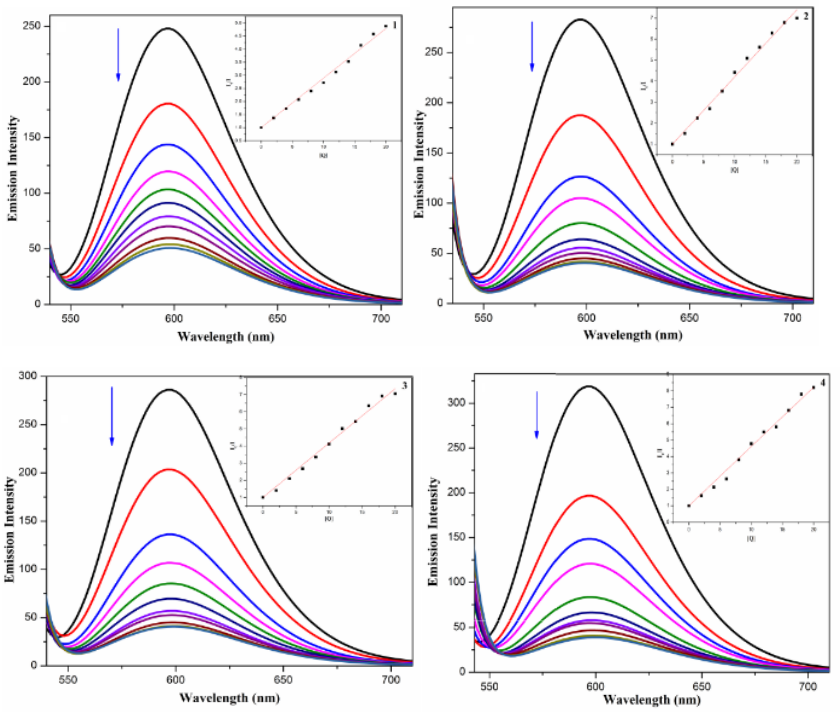

Fig. 4. Fluorescence quenching spectra depicting the titration of Ethidium Bromide bound DNA (Equimolar concentrations) vs complexes **1-4** (0-20 µM). The inset figure shows the Stern-Volmer plot and slope represents the quenching constant for the corresponding complex.

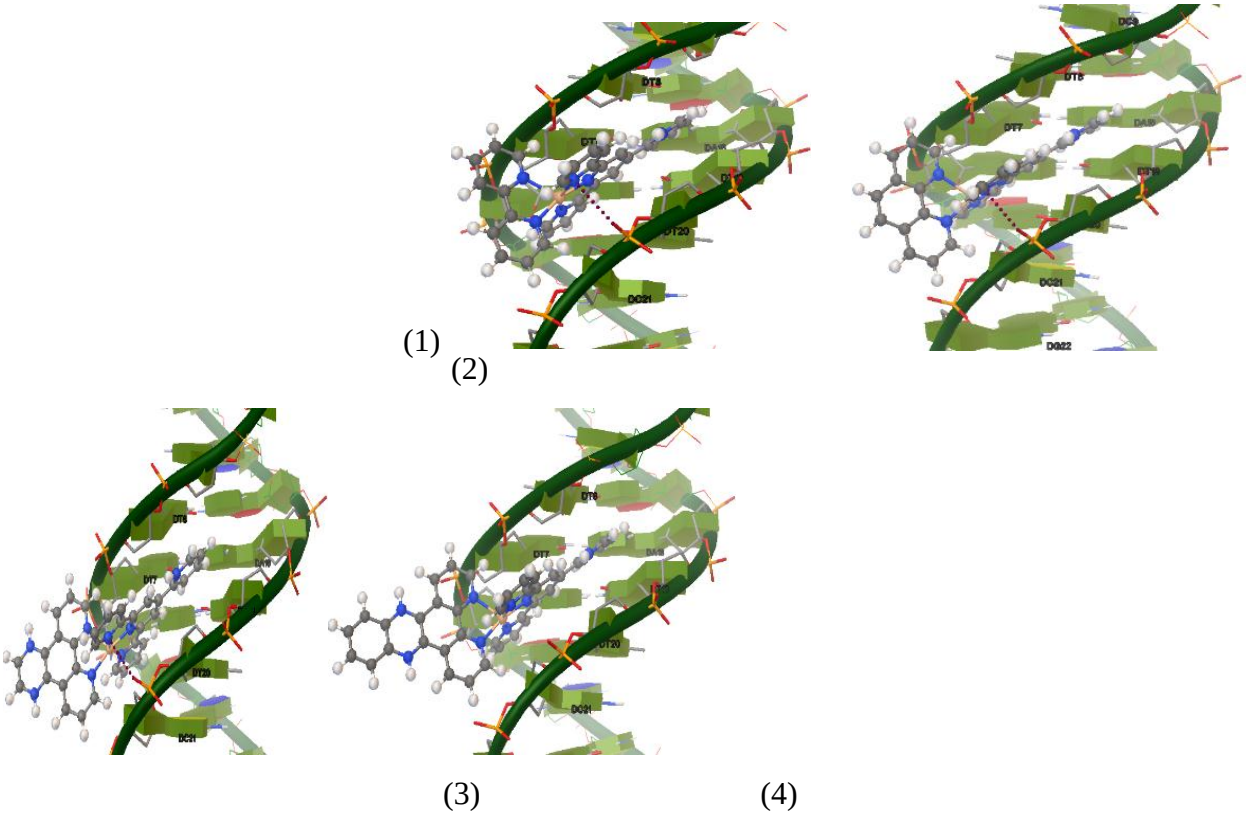

(1) (2)

(3) (4)

Fig. 5. Docked conformation of the complexes **1, 2 3** and **4** with crystal structure of ct-DNA (Pdb id: 355D). The complexes are represented in ball and stick model. The maroon dashed line represents the hydrogen bonds between the metal complexes and ct-DNA.

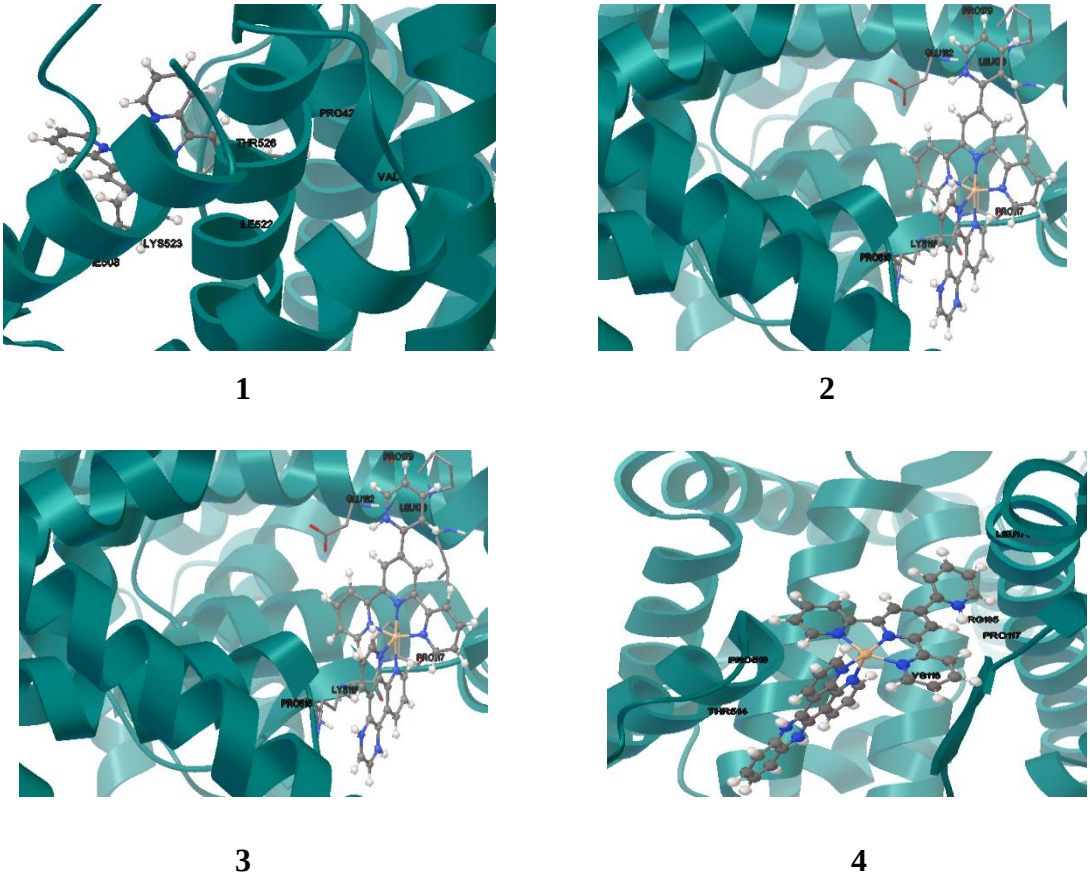

Fig. 6. Docked conformation of the complex **1-4** with crystal structure of Bovine serum albumin (PDB ID: 4JK4) is shown. The complexes are represented in ball and stick model. The interacting amino acids are given in black.

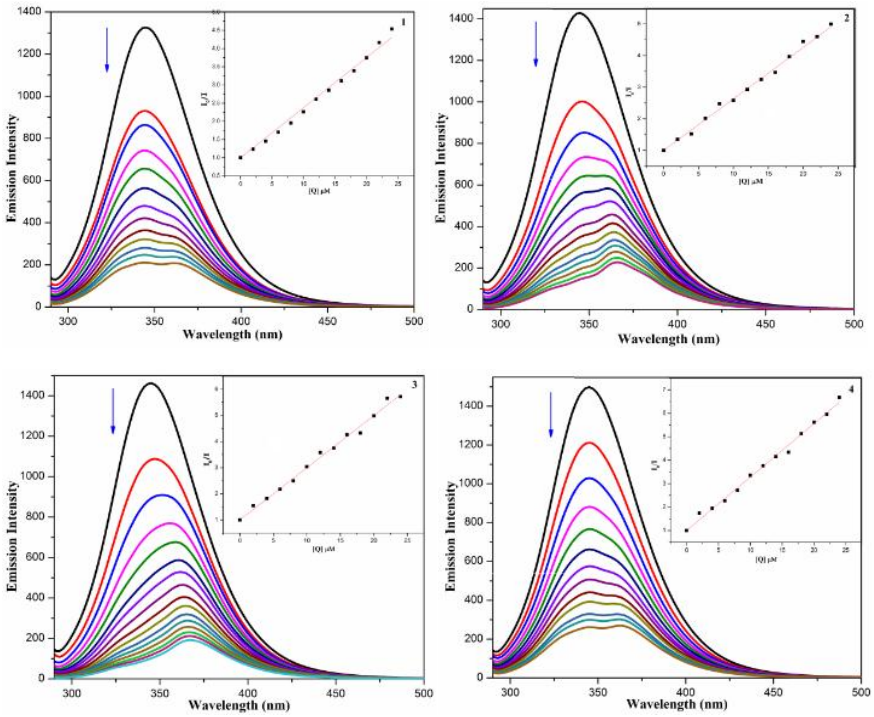

Fig. 7. The emission spectra of bovine serum albumin (BSA) with increasing concentration of metal complexes **1-4** (0-24 µM). The intrinsic fluorescence from BSA quenched with increasing concentration of metal complexes. The inset image shows the Stern-Volmer plot for the corresponding complex.

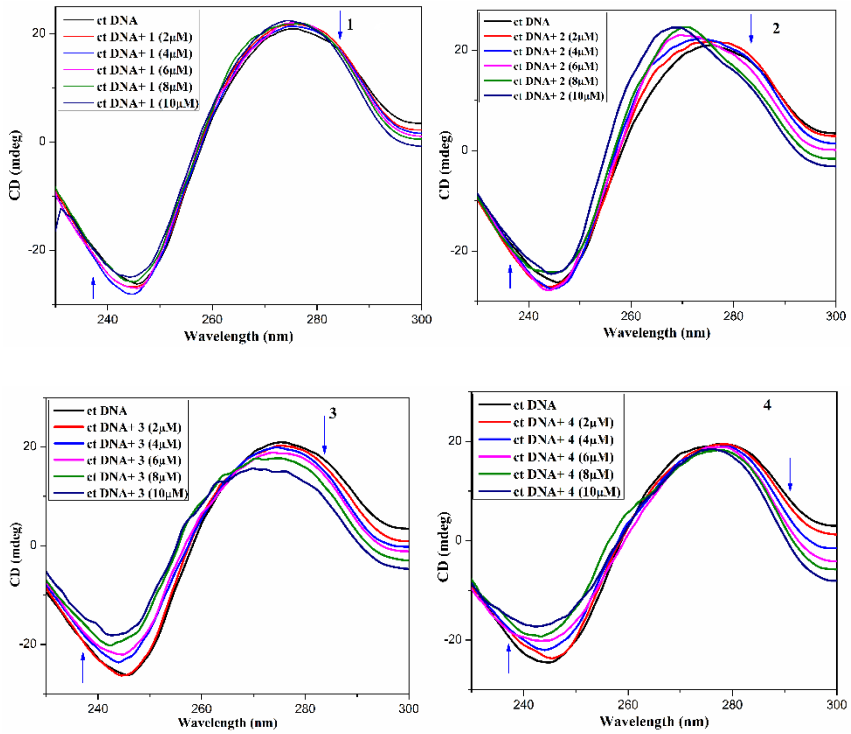

Fig. 8. The influence of metal complexes on the secondary structure of ct-DNA is revealed from the CD spectra. 100 μM of ct-DNA is titrated with increasing concentration of complexes **1-4** (0-12 μM).

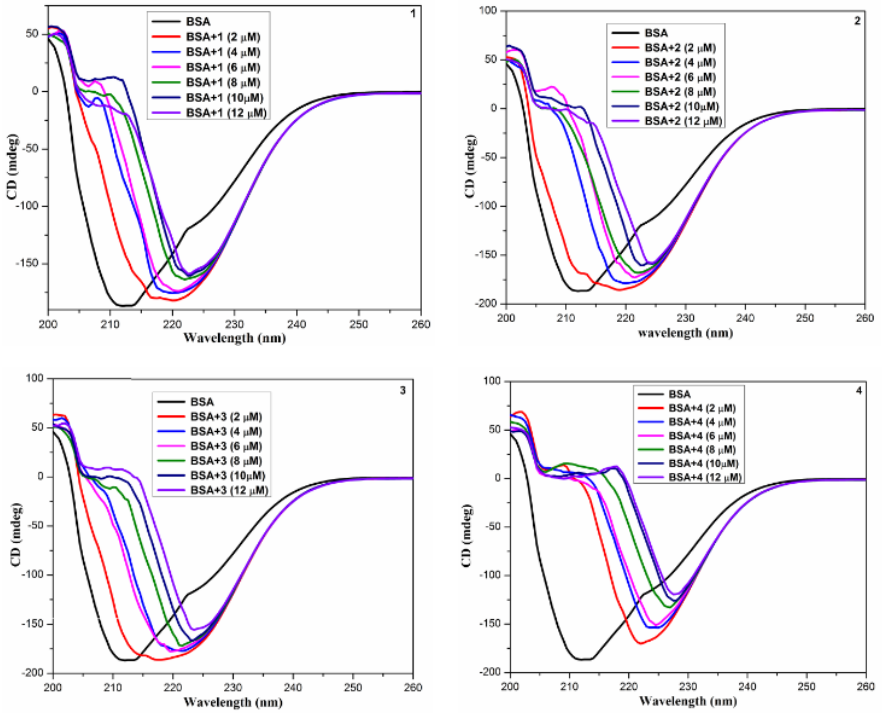

Fig. 9. Far UV secondary CD spectra of BSA indicating its interaction with metal complexes. 10 μM of BSA is titrated with increasing concentration of complexes **1-4** (0-12 μM).

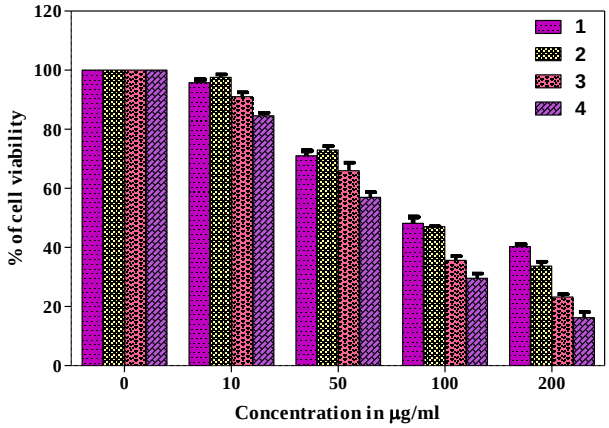

Fig. 10. Bar graph representing the cytotoxicity of metal complexes (**1-4**) as observed from MTT assay against human liver carcinoma cell line (HepG-2).

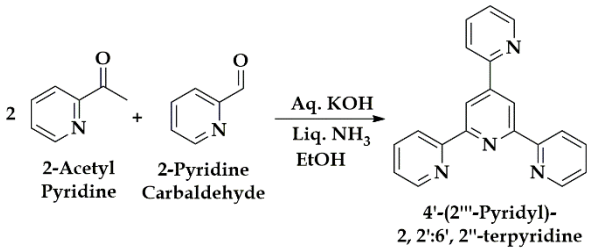

Scheme 1. Preparation of 4′-(2‴-Pyridyl)-2, 2′:6′, 2″-terpyridine.

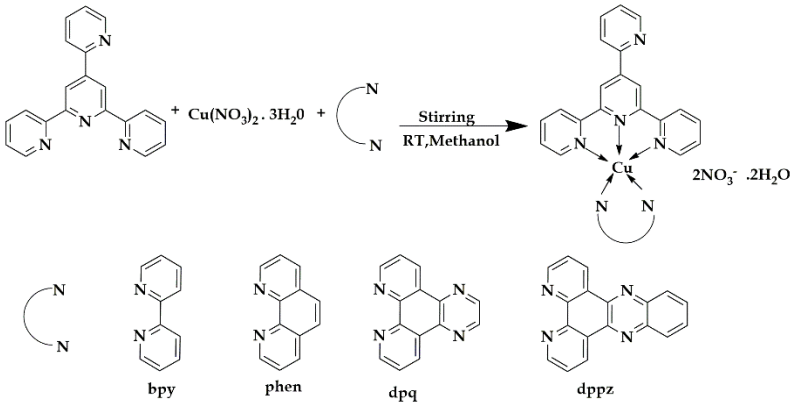

Scheme 2. Synthesis of new copper(II) derivatives.

List of Tables

Table 1 Comparison of computationally optimized molecular structure parameters (bond lengths (Å) and angles (°)) for complex **1-4** with the crystal structure data of complex **2**.

	Comp. B		**Comp. A**	**Comp. C**	**Comp. D**
	Exp.	**Cal.**	**Cal.**	**Cal.**	**Cal.**
Bond lengths (Å)					
Cu(1)-N(3)	2.060	2.1053	2.1029	2.1039	2.1056
Cu(1)-N(2)	1.932	1.9697	1.9700	1.9693	1.9703
Cu(1)-N(1)	2.055	2.1014	2.1071	2.1078	2.1091
Cu(1)-N(4)	1.999	2.0427	2.0431	2.0394	2.2627
Cu(1)-N(5)	2.278	2.2795	2.2501	2.2709	2.0378
Angles (°)					
N(1)- Cu(1)-N(2)	79.76	79.07	78.76	78.78	78.73
N(2)- Cu(1)-N(3)	79.60	78.80	79.03	79.04	78.99
N(3)- Cu(1)-N(4)	97.82	99.66	99.60	99.74	99.03
N(4)-Cu(1)-N(5)	78.21	78.37	77.38	78.36	78.51
N(5)-Cu(1)-N(1)	89.59	98.63	98.87	98.85	99.81
N(2)-Cu(1)-N(4)	176.38	165.91	164.92	167.20	167.15
N(4)-Cu(1)-N(1)	102.58	99.72	99.59	99.75	98.98
N(1)-Cu(1)-N(3)	158.83	156.28	156.19	155.83	155.66
N(2)-Cu(1)-N(5)	104.67	115.71	117.70	114.44	114.34
N(3)-Cu(1)-N(5)	100.16	98.57	98.97	98.95	99.71

Table 2 Binding energy (kcal/mol) and other non-covalent interaction energy values for DNA docked with four synthesized copper complexes (**1-4**).

Complexes	ΔG_{BE}	$\Delta G_{intermol}$		$\Delta G_{internal}$	ΔG_{tor}
		$\Delta G_{vdw\_hb\_desol}$	ΔG_{elec}		
1	−10.34	−10.65	0.01	−0.29	0.30
2	−10.21	−10.53	0.02	−0.29	0.30
3	−10.28	−10.59	0.01	−0.29	0.30
4	−10.28	−10.58	−0.04	−0.29	0.30

Table 3 The binding energy (ΔG_{BE}) intermolecular energy ($\Delta G_{intermol}$) of the complexes **1-4** with Bovine serum albumin protein is given below. All the energies are reported in kcal/mol.

Complexes	ΔG_{BE}	$\Delta G_{intermol}$		$\Delta G_{internal}$	ΔG_{tor}
		$\Delta G_{vdw\_hb\_desol}$	ΔG_{elec}		
1	−4.57	−4.85	−0.01	−0.27	0.30
2	−4.83	−5.08	−0.04	−0.28	0.30
3	−4.84	−5.13	−0.02	−0.29	0.30
4	−5.73	−5.94	−0.09	−0.28	0.30

Table 4 Protein binding constant (K_b), quenching constant (K_q) and number of binding sites (n) for complexes **1-4**.

Complex	K_b (M^{-1})	K_q (M^{-1})	n
1	1.06×10^6	1.83×10^5	1.02
2	2.19×10^6	2.53×10^5	1.18
3	3.38×10^6	2.86×10^5	1.32
4	4.76×10^6	3.40×10^5	1.39